Delay and Noise Formulas for Capacitively Coupled Distributed RC Lines

Hiroshi Kawaguchi

Institute of Industrial Science
University of Tokyo
Tokyo, Japan 106
Tel: +81-3-3403-1643
Fax: +81-3-3403-1649
Email: kawapy@cc.iis.u-tokyo.ac.jp

Takayasu Sakurai

Institute of Industrial Science
University of Tokyo
Tokyo, Japan 106
Tel: +81-3-3402-6231(ext. 2330)
Fax: +81-3-3402-3183
Email: tsakurai@iis.u-tokyo.ac.jp

Abstract— Simple yet useful analytical formulas for delay, slope and crosstalk noise amplitude for capacitively coupled two-, three- and infinite-line systems are derived assuming bus lines and other signal lines in deep-submicron VLSI's. The calculated results using the derived formulas are extensively compared with SPICE simulation results to demonstrate the validity of the analytical expressions. Two modes have been studied; the case where adjacent lines are driven from the opposite direction and the case where adjacent lines are driven from the same direction. These cases corresponds to the typical situations in VLSI designs and include worst cases in terms of noise amplitude and delay. Delay error in approximating the distributed RC lines by N-step π-ladder RC lumped circuit is also investigated.

1. Introduction

In deep submicron designs, interconnection related issues become more and more important in estimating timing behavior of VLSI's [1]. For instance, coupling capacitance is comparable to grounding capacitance. The coupling noise may cause malfunction and timing problem especially in dynamic circuits but even in static circuits, in addition, the noise may generate unexpected glitches which may give rise to timing and power problems.

Several attempts have been made to analytically treat the crosstalk in capacitively coupled interconnections. However, the results are limited to two-line systems and the case considered in the previous publications are limited to the case where adjacent lines are driven from the same direction. This paper extends the analysis and covers more general cases. The resultant formulas are more precise than the previously published expressions.

The delay of the RC distributed lines is also handled analytically in this paper. To the knowledge of the authors, formulas for the delay of the capacitively coupled distributed RC interconnection system have not been presented so rigorously and systematically as this paper. To analyze the capacitively coupled lines, moment matching technique based on Padé approximation is employed to give the analytical expressions.

The derived expressions are useful in estimating the noise and delay in the early stage of designs and give insight to coupling related issues.

2. Notations

Notations used in this paper are as follows.

c : capacitance of line per unit length.
C : total capacitance of line (=cl).
c_c : coupling capacitance of line per unit length.
C_C : total coupling capacitance of line (=c_cl).
C_t : equivalent capacitance of receiver MOSFET.
C_T : =C_t/C.
d : pure delay of voltage waveform.
E_i : step voltage of the driving point of line i (i=1,2). The condition that E_1=1, E_2=1 is called an in-phase drive. The condition that E_1=1, E_2=-1 is called an out-phase drive. The condition that E_1=1, E_2=0 is called E_2=0 drive.
K_1 : residue corresponding to σ_1.
l : line length.
m_k : k-th moment of voltage waveform k (k=0,1).
n : number of adjacent lines (n=1 for two-line system, n=2 for three-line system and n=1 for infinite-line system).
n_1 : =n+1.
p : =1+(n+1)η.
r : resistance of line per unit length.
R : total resistance of line (=rl).
R_t : equivalent resistance of driver MOSFET.
R_T : =R_t/R.
s : Laplace variable.
t : time.
t_p : time to give the noise peak.
t_{pd} : propagation delay using Padé approximation.
v_i, $v_i(x,t)$: voltage of line i (i=1,2) in t domain.
V_i, $V_i(x,s)$: voltage of line i (i=1,2) in s domain.
v_p : peak noise voltage.
x : x-coordinate along the line.
η : =C_C/C.
σ_1 : minimum absolute pole.
τ : time constant in single exponential approximation.

3. Basic Equations

The basic equations which governs a capacitively coupled two-line system (Fig. 1) are written as follows.

$$\begin{cases} \dfrac{\partial^2 v_1}{\partial x^2} = r_1(c_1 + c_c)\dfrac{\partial v_1}{\partial t} - r_1 c_c \dfrac{\partial v_2}{\partial t} \\ \dfrac{\partial^2 v_2}{\partial x^2} = r_2(c_2 + c_c)\dfrac{\partial v_2}{\partial t} - r_2 c_c \dfrac{\partial v_1}{\partial t} \end{cases} \quad (1)$$

, where r_i and c_i are resistance and capacitance of line i (i=1,2) per unit length. Since in bus structures and other wiring structures lines have the same resistance and capacitance per unit length, we assume $r_1=r_2=r$ and $c_1=c_2=c$.

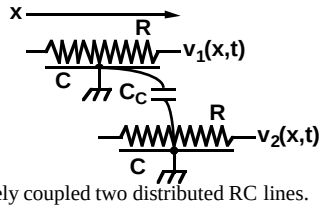

Fig. 1 Capacitively coupled two distributed RC lines.

When three-line system (Fig. 2) is considered, the following equations hold.

$$\begin{cases} \dfrac{\partial^2 v_1}{\partial x^2} = r(c + 2c_c)\dfrac{\partial v_1}{\partial t} - 2rc_c \dfrac{\partial v_2}{\partial t} \\ \dfrac{\partial^2 v_2}{\partial x^2} = r(c + c_c)\dfrac{\partial v_2}{\partial t} - rc_c \dfrac{\partial v_1}{\partial t} \end{cases} \quad (2)$$

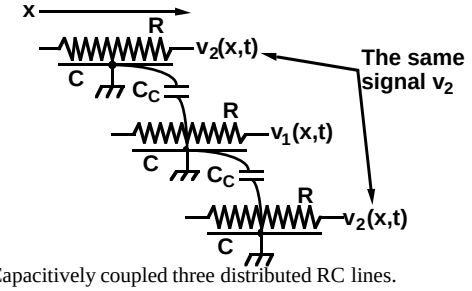

Fig. 2 Capacitively coupled three distributed RC lines.

On the other hand, if infinite lines are placed in parallel where the same boundary conditions are applied to every two lines as in Fig. 3, the following equations hold.

$$\begin{cases} \dfrac{\partial^2 v_1}{\partial x^2} = r(c + 2c_c)\dfrac{\partial v_1}{\partial t} - 2rc_c \dfrac{\partial v_2}{\partial t} \\ \dfrac{\partial^2 v_2}{\partial x^2} = r(c + 2c_c)\dfrac{\partial v_2}{\partial t} - 2rc_c \dfrac{\partial v_1}{\partial t} \end{cases} \quad (3)$$

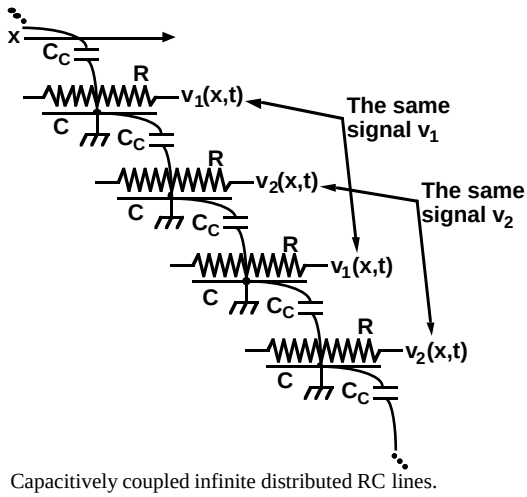

Fig. 3 Capacitively coupled infinite distributed RC lines.

All of the above-mentioned three equation sets (1), (2) and (3) can be represented by the following one set of equations.

$$\begin{cases} \dfrac{\partial^2 v_1}{\partial x^2} = r(c + nc_c)\dfrac{\partial v_1}{\partial t} - nrc_c \dfrac{\partial v_2}{\partial t} \\ \dfrac{\partial^2 v_2}{\partial x^2} = r(c + c_c)\dfrac{\partial v_2}{\partial t} - rc_c \dfrac{\partial v_1}{\partial t} \end{cases} \quad (4)$$

In the above equations (4), the following values should be set to n and c_c for each case.

Two-line case:	$n \to 1,\ c_c \to c_c$
Three-line case:	$n \to 2,\ c_c \to c_c$
Infinite-line case:	$n \to 1,\ c_c \to 2c_c$

(4) can be simplified, if the following substitutions are made.

$$t / rc \to \tilde{t},\ \ c_c / c \to \eta,\ \ \frac{\partial^2 v}{\partial x^2} \to v'',\ \ \frac{\partial v}{\partial \tilde{t}} \to \dot{v}$$

$$\begin{cases} v_1'' = (1 + n\eta)\dot{v}_1 - n\eta\dot{v}_2 \\ v_2'' = (1 + \eta)\dot{v}_2 - \eta\dot{v}_1 \end{cases}$$

are the resultant equations after the substitution. With a linear transformation, we have

$$\begin{cases} (v_1 + nv_2)'' = \dot{v}_1 + n\dot{v}_2 \\ (v_1 - v_2)'' = (1 + (n+1)\eta)(\dot{v}_1 - \dot{v}_2) \end{cases}$$

By Laplace transformation, the following equations can be derived.

$$\begin{cases} (V_1 + nV_2)'' = s(V_1 + nV_2) \\ (V_1 - V_2)'' = (1 + (n+1)\eta)s(V_1 - V_2) \end{cases}$$

The solutions of the above equations are expressed as follows with the introduction of γ_1 and γ_2.

$$\gamma_1 = \sqrt{s},\ \ \gamma_2 = \sqrt{(1 + (n+1)\eta)s} = \sqrt{ps}$$

$$\begin{cases} V_1 + nV_2 = A'e^{\gamma_1 x} + B'e^{-\gamma_1 x} \\ V_1 - V_2 = C'e^{\gamma_2 x} + D'e^{-\gamma_2 x} \end{cases}$$

, where A', B', C' and D' are integration constants.

$$\begin{cases} (n+1)V_1 = A'e^{\gamma_1 x} + B'e^{-\gamma_1 x} + nC'e^{\gamma_2 x} + nD'e^{-\gamma_2 x} \\ (n+1)V_2 = A'e^{\gamma_1 x} + B'e^{-\gamma_1 x} - C'e^{\gamma_2 x} - D'e^{-\gamma_2 x} \end{cases}$$

Then, the following are the general solutions to (4) in s-domain.

$$\begin{cases} V_1 = Ae^{\gamma_1 x} + Be^{-\gamma_1 x} + nCe^{\gamma_2 x} + nDe^{-\gamma_2 x} \\ V_2 = Ae^{\gamma_1 x} + Be^{-\gamma_1 x} - Ce^{\gamma_2 x} - De^{-\gamma_2 x} \end{cases} \quad (5)$$

A, B, C and D are to be obtained from boundary conditions.

A. Moment Matching Approach for Delay and Slope Calculation

Once A, B, C and D are obtained, closed-form expressions for $V_1(x,s)$ and $V_2(x,s)$ can be obtained using (5). Approximate voltage waveform of a full-swing line has an single exponential form with pure delay d shown in the following figure.

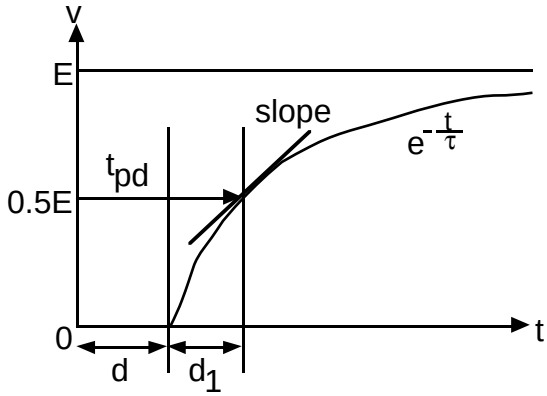

Fig. 4 Approximate voltage waveform of full-swing line.

In order to obtain expressions for the delay t_{pd}, the moment matching method (Padé approximation) is used [2-3], where the coefficients for s^0 and s^1 of the exact solution of (5) are matched to the coefficients of s^0 and s^1 of the approximate waveform in Fig. 4. The coefficient of s^0 is called the zero-th moment m_0 and the coefficient of s^1 is called the first moment m_1. m_0 happens to be the well-known Elmore delay. Taylor expansion of the approximate waveform in Fig. 4 is as follows.

$$\frac{1}{s} - m_0 + m_1 s + o[s^2] =$$

$$\frac{1}{s} - (\tau + d) + \left(\tau^2 + \tau d + \frac{d^2}{2}\right) s + o[s^2]$$

Consequently, once the moments of (5) are obtained, the delay t_{pd} and the slope of the waveform can be calculated as follows using Padé approximation.

$$\tau = \sqrt{2m_1 - m_0^2}, \quad d = m_0 - \tau$$

$$t_{pd} = d + d_1 = d + \tau \ln 2, \quad \text{slope}\big|_{t=tpd} = \frac{1}{2\tau} \tag{6}$$

In calculating the crosstalk noise, the moment matching approach is not effective because the noise shape varies from case to case and the assumption that the waveform is like Fig. 4 is not valid. For noise analysis, therefore, different approaches are taken from case to case.

4. Opposite Direction Drive

In this section, the mode where adjacent lines are driven from the opposite direction is handled. The situation is depicted in Fig. 5. For this mode, analytical expressions turn out to be very complicated if the equivalent resistance of driver MOSFET R_t and the equivalent capacitance of receiver MOSFET C_t are to be considered, that is, R_T and C_T are not equal to zero. The case of R_T=C_T=0, however, gives the worst case scenario in terms of the noise amplitude because the capacitance coupling effect is mitigated if R_T and C_T are finite. Consequently, the R_T=C_T=0 case is treated here.

The boundary conditions for this case are as follows (Fig. 5).

$$\begin{cases} V_1'(0,s) = 0 \\ V_1(l,s) = E_1/s \\ V_2(0,s) = E_2/s \\ V_2'(l,s) = 0 \end{cases}$$

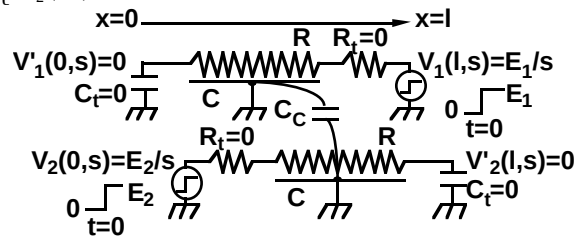

Fig. 5 Adjacent lines are driven from the opposite direction (R_t=C_t=0).

Writing these conditions using (5) yields

$$\begin{cases} A\gamma_1 - B\gamma_1 + nC\gamma_2 - nD\gamma_2 = 0 \\ Ae^{\gamma_1 l} + Be^{-\gamma_1 l} + nCe^{\gamma_2 l} + nDe^{-\gamma_2 l} = E_1/s \\ A + B - C - D = E_2/s \\ A\gamma_1 e^{\gamma_1 l} - B\gamma_1 e^{-\gamma_1 l} - C\gamma_2 e^{\gamma_2 l} + D\gamma_2 e^{-\gamma_2 l} = 0 \end{cases}$$

The above linear equations can be solved in terms of A, B, C and D. Then A, B, C and D are substituted back in (5) and the closed-form expressions for $V_1(x,s)$ and $V_2(x,s)$ are obtained.

A. Crosstalk Noise

Although the derived expression for $V_1(x,s)$ is very complicated, the peak noise amplitude, v_{p1}, can be calculated using the following initial value theorem of Laplace transform. In order to obtain the crosstalk noise on $V_1(x,s)$, E_1 is set to 0 and E_2 is set to E.

$$\frac{v_{p1}}{E} = \frac{v_1(0,+0)}{E} = \frac{\lim_{s\to\infty} sV_1(0,s)}{E}$$

The resultant expression for the peak noise amplitude is simple as follows. The formulas are exact. Special case expressions for two-, three- and infinite-line systems are also shown.

$$\begin{cases} \dfrac{v_{p1}}{E} = \dfrac{n\sqrt{1+(n+1)\eta} - n}{n\sqrt{1+(n+1)\eta} + 1} & \text{(general, exact)} \\ \dfrac{v_{p1}}{E} = \dfrac{\sqrt{1+2C_c/C} - 1}{\sqrt{1+2C_c/C} + 1} & \text{(two-line)} \\ \dfrac{v_{p1}}{E} = \dfrac{2\sqrt{1+3C_c/C} - 2}{2\sqrt{1+3C_c/C} + 1} & \text{(three-line)} \\ \dfrac{v_{p1}}{E} = \dfrac{\sqrt{1+4C_c/C} - 1}{\sqrt{1+4C_c/C} + 1} & \text{(infinite-line)} \end{cases} \tag{7}$$

If the coupling capacitance C_C is equal to the grounding capacitance C, which can happened in deep submicron designs, v_{p1}/E for two-, three- and infinite-line systems are 0.27, 0.40 and 0.38, respectively. This means that the noise induced by the coupling would go up to 40% of the signal swing, which may in turn cause malfunction and timing

problems. This situation can be verified by SPICE [4] simulation results as seen in Fig. 6. The SPICE simulation is carried out by using 10 sections of lumped RC blocks.

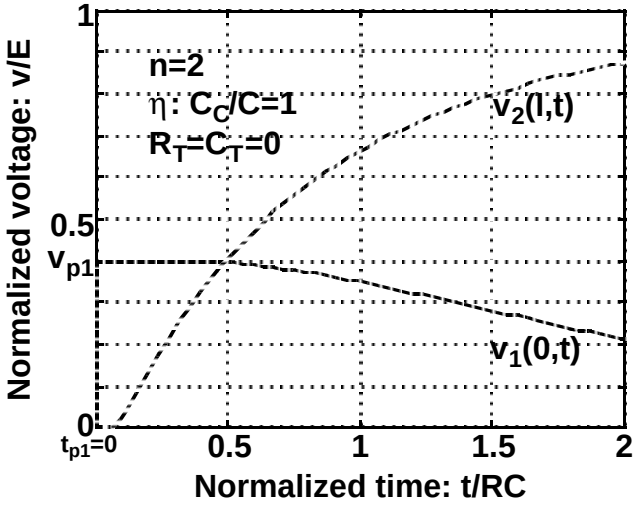

Fig. 6 SPICE simulation results for the case where adjacent lines are driven from the opposite direction (three-line system).

B. Delay and Slope

Although the expressions for voltage waveform, $V_1(x,s)$ and $V_2(x,s)$ are also complicated, the moments, m_0 and m_1 of $V_1(0,s)$ can be expressed as below. Once m_0 and m_1 are obtained, the delay t_{pd} and the slope are calculated using (6).

$$\begin{cases} m_0 / RC = \frac{1}{2}\{E_1(1+n\eta) - E_2 n\eta\} \\ m_1 / (RC)^2 = \frac{1}{24}[E_1\{(5+5n^2\eta^2 + n\eta(10+3\eta)\} \\ \qquad -E_2 n\eta\{8+(3+5n)\eta\}] \end{cases} \tag{8}$$

The worst case in terms of delay occurs when n=2 and the adjacent lines are driven in out-phase fashion, that it, E_1=1 and E_2=-1. t_{pd} in this worst case is expressed as follows.

$$\frac{t_{pd}}{RC} = \frac{1}{2} + 2\eta - \frac{1}{\sqrt{6}}\log\frac{e}{2}\sqrt{1+6\eta+2\eta^2} \approx 1.7\eta + 0.37 \quad (\eta \le 2) \tag{9}$$

Typical delay simulation example is shown in Fig. 7.

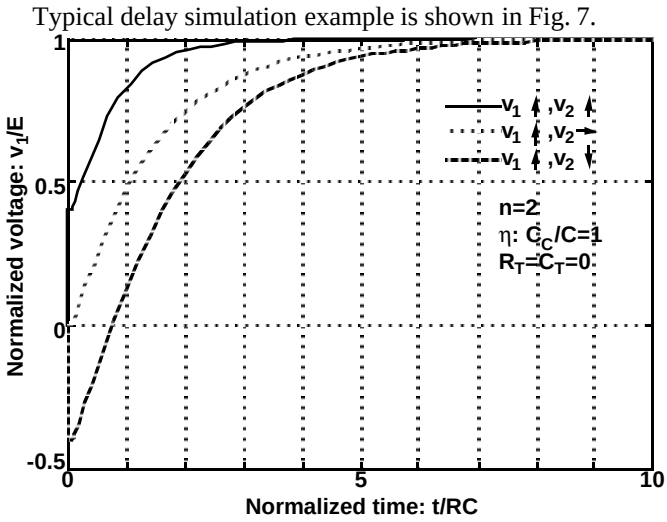

Fig. 7 Delay simulation example for the opposite drive case (three-line system).

5. Same Direction Drive

In this section, the mode where adjacent lines are driven from the same direction is treated. The situation is depicted in Fig. 8. For this case, the equivalent resistance of driver MOSFET R_t and the equivalent capacitance of receiver MOSFET C_t can be taken into account in the analysis, that is, R_T and C_T can be finite.

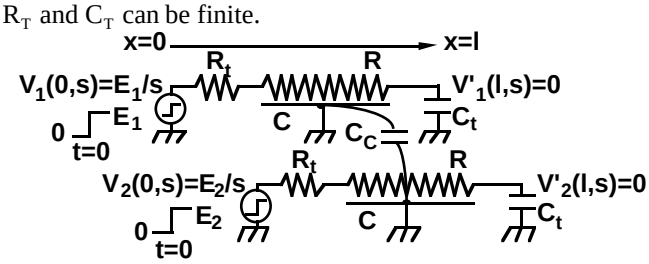

Fig. 8 Adjacent lines are driven from the same direction.

The boundary conditions for this case are written as follows.

$$\begin{cases} -\frac{1}{r}\frac{\partial v_1}{\partial x}\Big|_{x=0} = \frac{E_1 - v_1}{R_t}\Big|_{x=0} \\ -\frac{1}{r}\frac{\partial v_1}{\partial x}\Big|_{x=1} = C_t\frac{\partial v_1}{\partial t}\Big|_{x=1} \\ -\frac{1}{r/n}\frac{\partial v_2}{\partial x}\Big|_{x=0} = \frac{E_2 - v_2}{R_t/n}\Big|_{x=0} \\ -\frac{1}{r/n}\frac{\partial v_2}{\partial x}\Big|_{x=1} = nC_t\frac{\partial v_2}{\partial t}\Big|_{x=1} \end{cases} \tag{10}$$

A. Crosstalk Noise

In order to obtain the crosstalk noise, the moment matching approach is not effective and a special analytical treatment like below is employed. For noise calculation, E_1 is set to 0 and E_2 is set to E.

If we define $u_1=v_1+nv_2$ and $u_2=v_1-v_2$, u_1 and u_2 give the following equations.

$$\begin{cases} \frac{\partial^2 u_1}{\partial x^2} = rc\frac{\partial u_1}{\partial t} \\ \frac{\partial^2 u_2}{\partial x^2} = prc\frac{\partial u_2}{\partial t} = rc\frac{\partial u_2}{\partial (t/p)} = rc\frac{\partial u_2}{\partial t'} \end{cases} \tag{11}$$

The boundary conditions for u_1 and u_2 are obtained by linearly combining (10) as follows.

$$\begin{cases} -\frac{1}{r}\frac{\partial u_1}{\partial x}\Big|_{x=0} = \frac{nE - u_1}{R_t}\Big|_{x=0} \\ -\frac{1}{r}\frac{\partial u_1}{\partial x}\Big|_{x=1} = C_t\frac{\partial u_1}{\partial t}\Big|_{x=1} \\ -\frac{1}{r}\frac{\partial u_2}{\partial x}\Big|_{x=0} = \frac{-E - u_2}{R_t}\Big|_{x=0} \\ -\frac{1}{r}\frac{\partial u_2}{\partial x}\Big|_{x=1} = \frac{C_t}{p}\frac{\partial u_2}{\partial t'}\Big|_{x=1} \end{cases} \tag{12}$$

On the other hand, it is well-known that the equation

$$\frac{\partial^2 v}{\partial x^2} = rc\frac{\partial v}{\partial t}$$

with the boundary condition,

$$\begin{cases} -\frac{1}{r}\frac{\partial v}{\partial x}\Big|_{x=0} = \frac{E-v}{R_t}\Big|_{x=0} \\ -\frac{1}{r}\frac{\partial v}{\partial x}\Big|_{x=1} = C_t\frac{\partial v}{\partial t}\Big|_{x=1} \end{cases}$$

has the following solution [5-7].

$$\frac{v(l,t)}{E} = 1 + \sum_{k=1}^{\infty} K_k e^{\frac{-\sigma_k t}{RC}} \approx 1 + K_1 e^{\frac{-\sigma_1 t}{RC}}$$

This means that v(l,t) can be approximated with a single exponential function. σ_1 is the pole with minimum absolute value, and K_1 is the corresponding residue and can be approximated as follows.

$$\begin{cases} K_1 \approx -1.01\frac{R_T + C_T + 1}{R_T + C_T + \pi/4} \\ \sigma_1 \approx \frac{1.04}{R_T C_T + R_T + C_T + (2/\pi)^2} \end{cases}$$

Comparing the above solved system and (11) and (12), we get approximate formulas for u_1 and u_2. v_1 and v_2 are obtained by a linear combination of u_1 and u_2 as follows.

$$\begin{cases} \frac{v_1(l,t)}{E} \approx \frac{n}{n+1}\left(K_1 e^{-\frac{\sigma_1 t}{RC}} - K_1' e^{-\frac{\sigma_1' t}{pRC}}\right) \\ \frac{v_2(l,t)}{E} \approx 1 + \frac{1}{n+1}\left(K_1 e^{-\frac{\sigma_1 t}{RC}} + nK_1' e^{-\frac{\sigma_1' t}{pRC}}\right) \end{cases} \quad (13)$$

In the above expression, K_1' and σ_1' are expressed as follows.

$$\begin{cases} K_1' \approx -1.01\frac{R_T + C_T/p + 1}{R_T + C_T/p + \pi/4} \\ \sigma_1' \approx \frac{1.04}{R_T C_T/p + R_T + C_T/p + (2/\pi)^2} \end{cases}$$

The peak noise amplitude can be derived by searching for the peak value in (13). This can be achieved by differentiating (13) and solve $\partial v_1/\partial t=0$ in terms of t. If we write the solution to this equation as t_{p1}, t_{p1} can be expressed as follows.

$$t_{p1} = \frac{p\ln\left(\frac{K_1\sigma_1}{K_1'\sigma_1'}p\right)}{p\sigma_1 - \sigma_1'}$$

Now, putting t_{p1} back in (13), the peak noise amplitude is obtained.

$$\frac{v_{p1}}{E} \approx \frac{n}{n+1}\left[K_1\left(\frac{K_1\sigma_1}{K_1'\sigma_1'}p\right)^{\frac{p\sigma_1}{-p\sigma_1+\sigma_1'}} - K_1'\left(\frac{K_1\sigma_1}{K_1'\sigma_1'}p\right)^{\frac{\sigma_1'}{-p\sigma_1+\sigma_1'}}\right] \quad (14)$$

Several special cases are discussed in the following chapters.

A-1. Noise for the Case: R_T,C_T»1

In this case, $K_1=K_1'\approx-1$, $\sigma_1\approx1/(R_TC_T)$ and $\sigma_1'\approx p/(R_TC_T)$ hold. Then, from (14), $v_{p1}\to0$. This case corresponds to the old situation where interconnection capacitance and resistance are not large compared to MOSFET related resistance and capacitance. For this case, as a matter of course, noise issues can be neglected. The capacitance coupling noise is rather a new headache in VLSI designs.

A-2. Noise for the Case: R_T,C_T«1

In this case, $K_1=K_1'\approx-4/\pi$ and $\sigma_1=\sigma_1'\approx\pi^2/4$ hold.

$$v_{p1} \approx \frac{4}{\pi}n\left(\frac{1}{1+n_1\eta}\right)^{\frac{1}{n_1\eta}}\frac{\eta}{1+n_1\eta}$$

$$\approx \frac{n\eta}{2+(n+1)\eta} \text{ (valid when } \eta \le 2)$$

Special case expressions for two-, three- and infinite-line systems are shown below.

$$\begin{cases} \frac{v_{p1}}{E} \approx \frac{nC_c/C}{2+(n+1)C_c/C} & \text{(general)} \\ \frac{v_{p1}}{E} \approx \frac{C_c/C}{2+2C_c/C} & \text{(two-line)} \\ \frac{v_{p1}}{E} \approx \frac{2C_c/C}{2+3C_c/C} & \text{(three-line)} \\ \frac{v_{p1}}{E} \approx \frac{C_c/C}{1+2C_c/C} & \text{(infinite-line)} \end{cases} \quad (15)$$

The approximation is valid when $C_C/C\le2$. If the coupling capacitance C_C is equal to the grounding capacitance C which can happened in deep submicron designs, v_{p1}/E for two-, three- and infinite-line systems are 0.25, 0.40 and 0.33, respectively. This means that the noise induced by the coupling would go up to 40% of the signal swing, which is the same situation as in the previous section. This situation can be verified by the SPICE simulation as seen in Fig. 9.

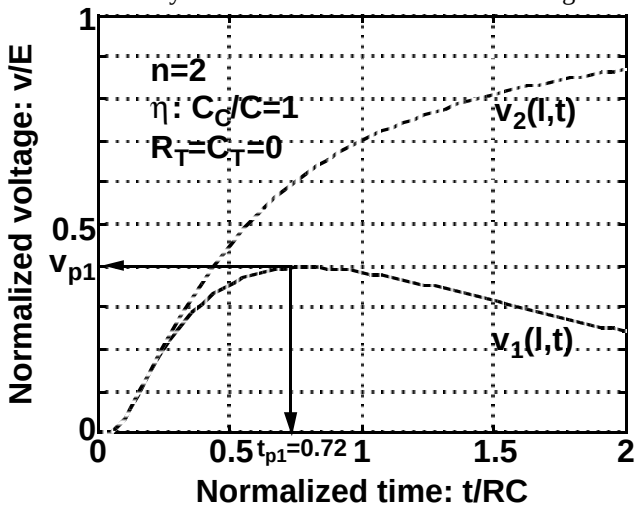

Fig. 9 SPICE simulation results for the case where adjacent lines are driven from the same direction (three-line system).

For this case, the time when the noise shows the peak t_{p1} is approximated as follows.

$$\frac{t_{p1}}{RC} \approx \frac{4}{\pi^2}\frac{p\ln p}{p-1}$$

A-3. Noise for the Case: C_T«1

This is similar to the previous case and the noise amplitude is approximated as follows.

$$v_{p1} \approx \frac{R_T+1}{R_T+\frac{\pi}{4}}\eta\left(\frac{1}{1+n_1\eta}\right)^{\frac{1}{n_1\eta}}\frac{\eta}{1+n_1\eta}$$

$$\approx \frac{R_T+1}{1.27R_T+1}\frac{n\eta}{2+(n+1)\eta} \text{ (valid when } \eta \le 2)$$

A-4. Noise for the Case: R_T»1

In this case,

$$v_{p1} \approx n\left(\frac{1}{1+n_1\eta'}\right)^{\frac{1}{n_1\eta'}}\frac{\eta'}{1+n_1\eta'}$$

$$\approx 0.80\frac{n\eta'}{2+(n+1)\eta'} \text{ (valid when } \eta' \le 2)$$

, where $\eta'=C_C/(C+Ct)$.

B. Delay and Slope

Although the expressions for voltage waveform are complicated, the moments, m_0 and m_1 of $V_1(l,s)$ can be expressed as below. Once m_0 and m_1 are obtained, the delay t_{pd} and the slope are calculated using (6).

$$\begin{cases} m_0 / RC = \frac{1}{2}[E_1\{2C_T(1+R_T)+(1+2R_T)(1+n\eta)\} \\ \quad -E_2 n\eta(1+2R_T)] \\ m_1/(RC)^2 = \frac{1}{24}[E_1\{24C_T^2(1+R_T)^2 \\ \quad +4C_T(5+15R_T+12R_T^2)(1+n\eta) \\ \quad +(5+20R_T+24R_T^2)(1+2n\eta+n\eta^2+n^2\eta^2)\} \\ \quad -E_2\eta\{4C_T((2+3n)(1+3R_T)+6(1+n)R_T^2) \\ \quad +(5+20R_T+24R_T^2)(2+\eta+n\eta)\}] \end{cases} \quad (16)$$

The worst case in terms of delay occurs when n=2 and the adjacent lines are driven in out-phase fashion, that it, E_1=1 and E_2=-1. A simple case when C_T=R_T=0, t_{pd} in this worst case is expressed as follows.

$$\frac{t_{pd}}{RC} = \frac{1}{2}+2\eta-\frac{1}{\sqrt{6}}\log\frac{e}{2}\sqrt{1+8\eta+6\eta^2} \quad (17)$$

$$\approx 1.63\eta+0.37 \ (\eta \le 2)$$

Typical delay simulation example is shown in Fig. 10. It is seen from the figure that t_{pd} in three-line system varies from 0.37RC (in-phase) to 2.0RC (out-phase) depending on the behavior of the adjacent lines. When E_2=0, t_{pd} is 0.98RC.

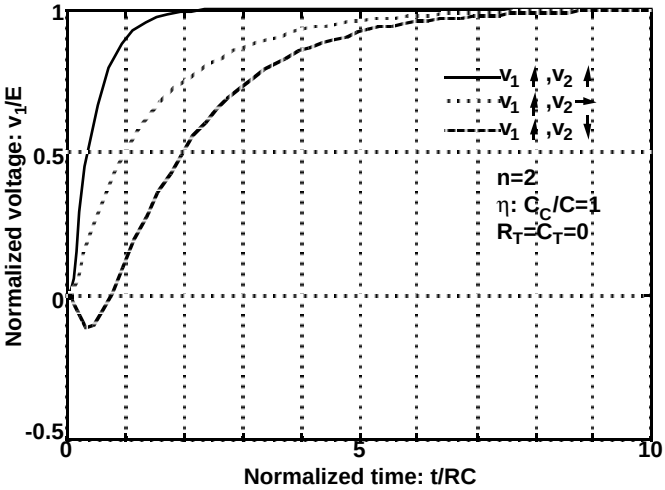

Fig. 10 Delay simulation example for the same direction drive case (three-line system).

6. Comparison with Simulation

A. Crosstalk Noise

SPICE simulation is carried out to demonstrate the validity of the noise peak formulas of (7) and (14). The simulation results are compared with the calculated results using the analytical formulas in Figs. 11, 12 and 13. As seen from the figures, excellent agreement is observed between the simulated and the calculated results.

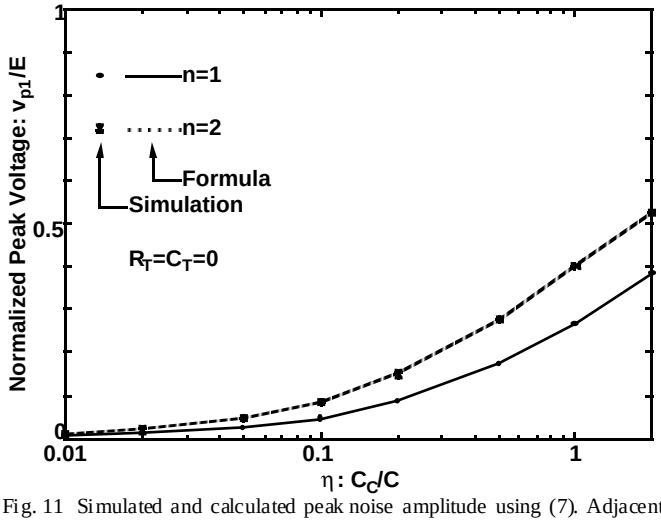

Fig. 11 Simulated and calculated peak noise amplitude using (7). Adjacent lines are driven from the opposite direction.

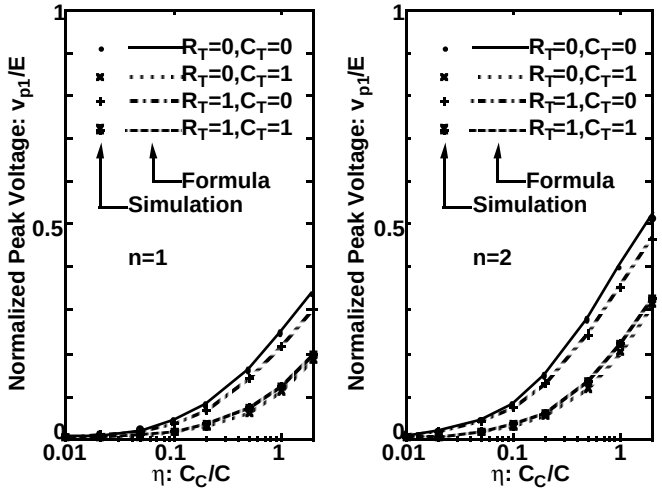

Fig. 12 Simulated and calculated peak noise amplitude using (14). Adjacent lines are driven from the same direction.

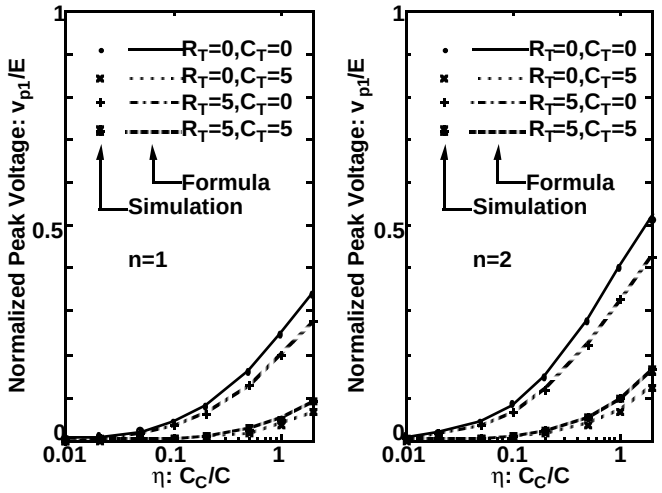

Fig. 13 Simulated and calculated peak noise amplitude using (14). Adjacent lines are driven from the same direction.

B. Delay and Slope

The simulation results for delay and slope are compared with the calculated results using the analytical formulas (6), (8) and (16) in Fig. 14 through Fig. 21. As seen from the figures, good agreement is observed between the simulated and the calculated results.

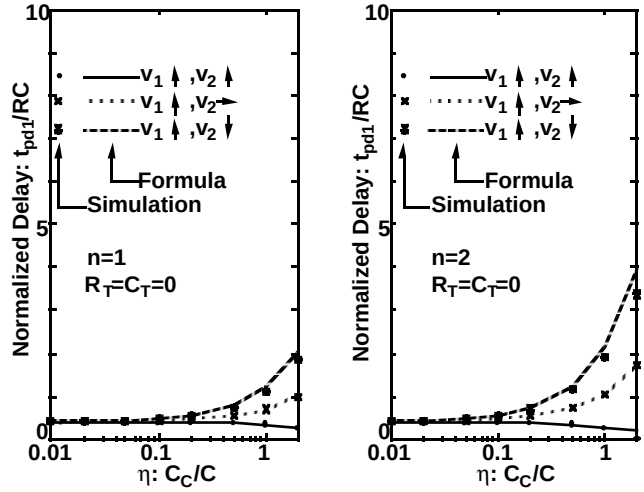

Fig. 14 Simulated and calculated delay using (6) and (8). Adjacent lines are driven from the opposite direction.

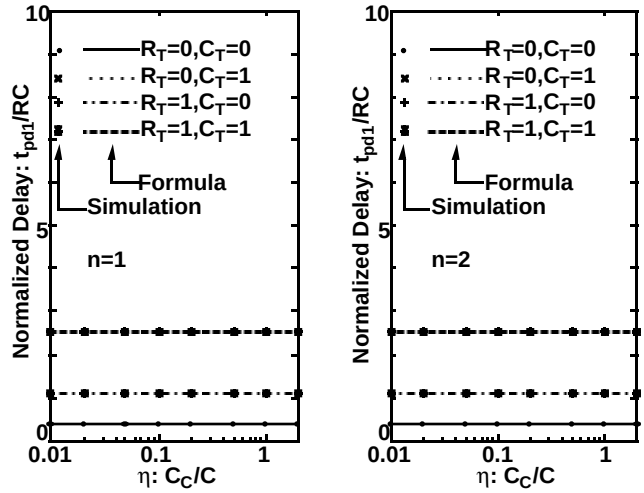

Fig. 15 Simulated and calculated delay using (6) and (16). The case is for the same direction and in-phase drive.

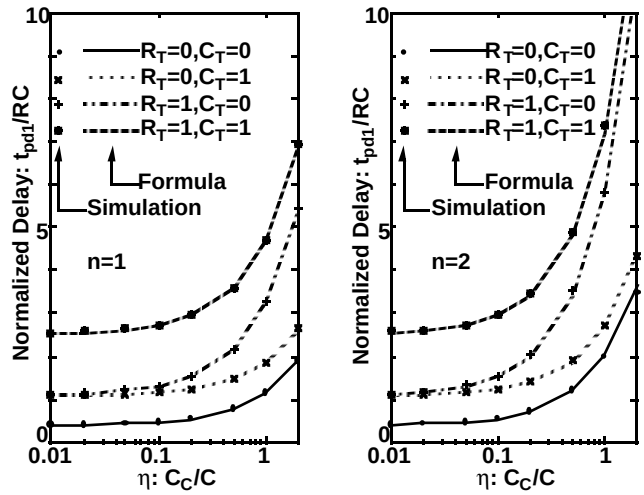

Fig. 16 Simulated and calculated delay using (6) and (16). The case is for the same direction and out-phase drive.

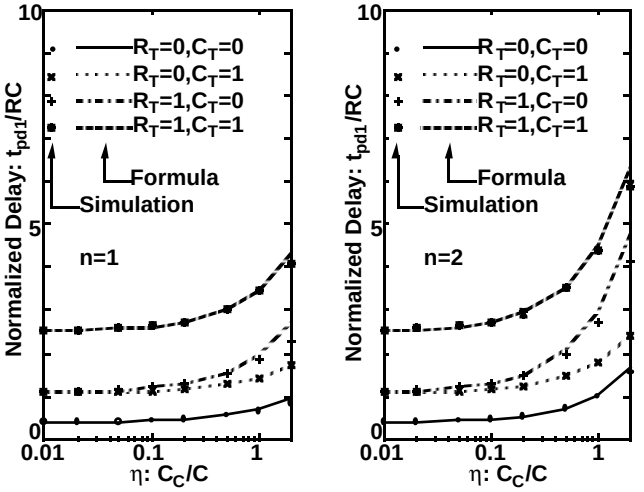

Fig. 17 Simulated and calculated delay using (6) and (16). The case is for the same direction and E_2=0 drive.

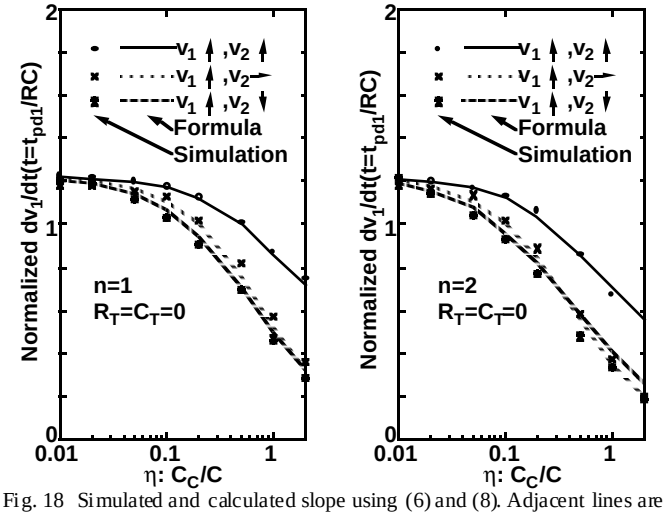

Fig. 18 Simulated and calculated slope using (6) and (8). Adjacent lines are driven from the opposite direction.

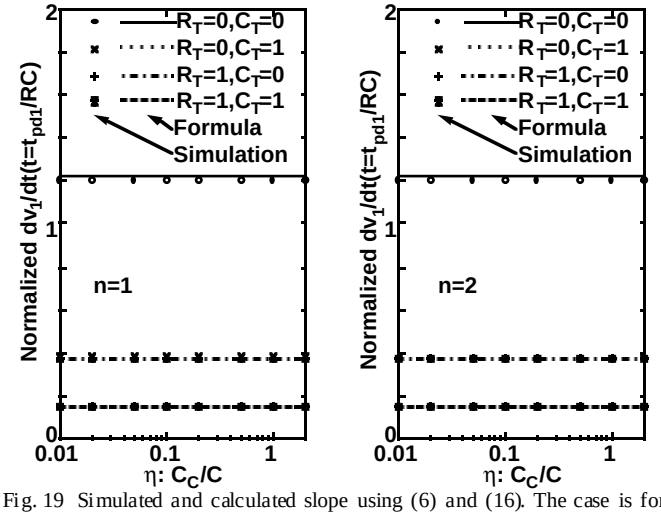

Fig. 19 Simulated and calculated slope using (6) and (16). The case is for the same direction and in-phase drive.

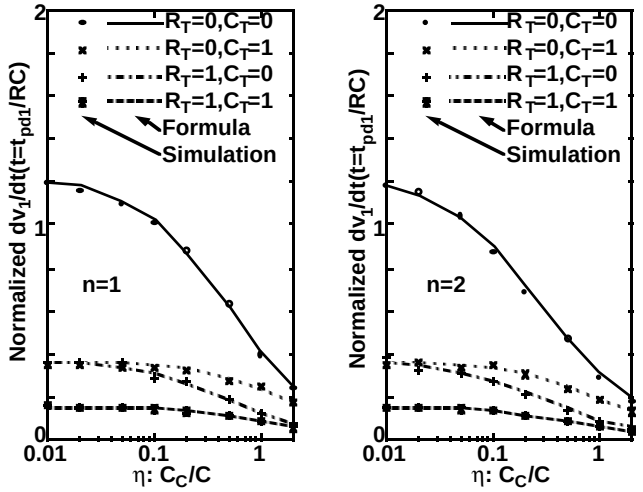

Fig. 20 Simulated and calculated slope using (6) and (16). The case is for the same direction and out-phase drive.

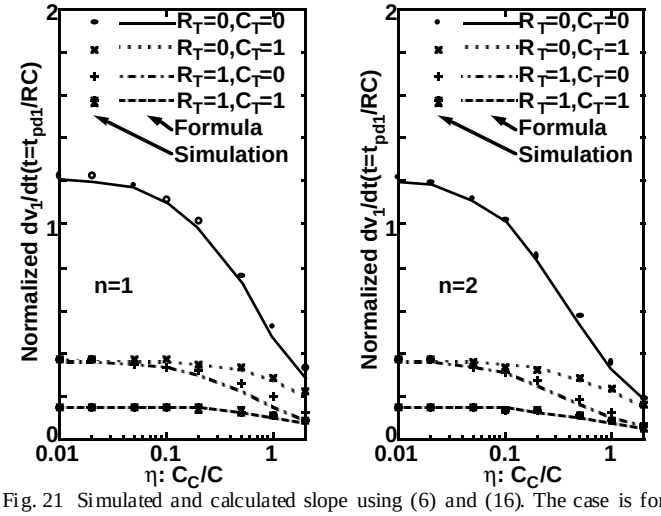

Fig. 21 Simulated and calculated slope using (6) and (16). The case is for the same direction and E_2=0 drive.

7. Approximation with Lumped Circuit

In circuit simulation, π-ladder lumped circuit is often adopted to approximate the distributed RC lines. The error in simulating delay of the distributed RC line by using N-step lumped ladder blocks (Fig. 22) is investigated.

The results are shown in TABLE 1 through TABLE 6. Numbers in the tables signify % error of the delay. The reference (exact delay) is taken from the simulation results with N=10. C_T and R_T are set equal to 0, because this condition corresponds to the worst case in terms of error. When C_T and R_T are finite, they tend to determine the timing behavior of the system and they are lumped circuit elements from first.

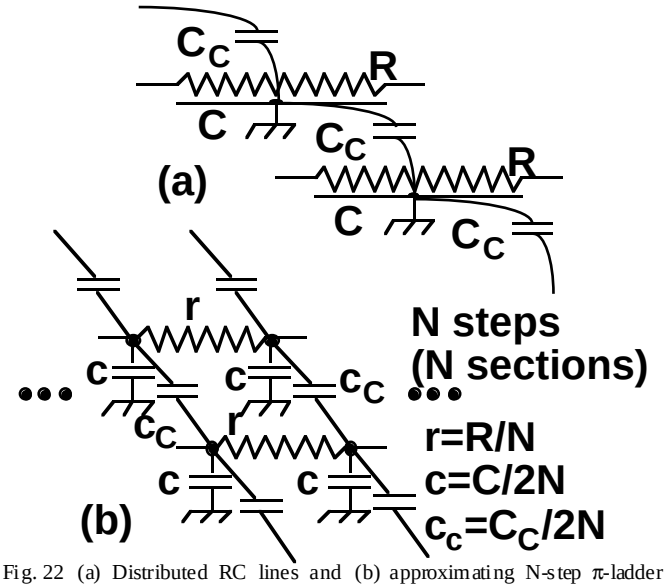

Fig. 22 (a) Distributed RC lines and (b) approximating N-step π-ladder circuit.

It is seen from these tables that 3-step π-ladder network is a good approximation in estimating delay within 4% relative error even in the worst cases.

TABLE 1 Delay % error with lumped circuit (opposite direction, in-phase drive case)

	n=1				n=2			
η	N=1	N=2	N=3	N=5	N=1	N=2	N=3	N=5
0.01	8.9	1.0	0.3	0.1	9.4	1.0	0.3	0.1
0.1	13.2	1.1	0.3	0.1	19.0	1.4	0.3	0.1
0.4	33.0	2.5	0.6	0.1	73.6	7.1	1.6	0.4
1	–	–	–	–	–	–	–	–
4	–	–	–	–	–	–	–	–

– signifies that the relative error can not be calculated because the exact delay is zero but the absolute error is smaller than 0.001RC.

TABLE 2 Delay % error with lumped circuit (opposite direction, out-phase drive case)

	n=1				n=2			
η	N=1	N=2	N=3	N=5	N=1	N=2	N=3	N=5
0.01	8.3	1.4	0.8	0.1	7.0	0.5	-0.9	-0.9
0.1	5.5	1.0	0.4	0.4	4.5	1.6	0.9	0.3
0.4	2.1	1.7	0.6	0.2	3.7	1.7	0.6	0.0
1	1.0	1.9	0.8	0.2	4.9	1.8	0.7	0.2
4	2.4	3.0	1.3	0.4	5.0	1.2	0.4	0.1

TABLE 3 Delay % error with lumped circuit (opposite direction, E_2=0 drive case)

	n=1				n=2			
η	N=1	N=2	N=3	N=5	N=1	N=2	N=3	N=5
0.01	8.3	0.9	0.1	0.0	8.3	0.9	0.1	0.0
0.1	8.4	0.9	0.3	0.1	7.9	0.8	0.2	0.0
0.4	6.0	0.7	0.1	0.0	5.5	0.6	0.2	0.0
1	0.5	0.1	-0.1	0.0	2.1	0.6	0.2	0.0
4	-15.6	-1.9	-0.3	0.0	-0.4	1.8	0.8	0.2

TABLE 4 Delay % error with lumped circuit (same direction, in-phase drive case)

	n=1				n=2			
η	N=1	N=2	N=3	N=5	N=1	N=2	N=3	N=5
0.01	8.5	0.9	0.3	0.1	8.5	0.9	0.3	0.1
0.1	8.5	0.9	0.3	0.1	8.5	0.9	0.3	0.1
0.4	8.5	0.9	0.3	0.1	8.5	0.9	0.3	0.1
1	8.5	0.9	0.3	0.1	8.5	0.9	0.3	0.1
4	8.5	0.9	0.3	0.1	8.5	0.9	0.3	0.1

TABLE 5 Delay % error with lumped circuit (same direction, out-phase drive case)

	n=1				n=2			
η	N=1	N=2	N=3	N=5	N=1	N=2	N=3	N=5
0.01	8.6	1.6	0.0	0.0	8.8	1.7	1.3	0.0
0.1	8.2	0.5	0.2	-0.4	8.4	1.4	0.5	0.6
0.4	8.4	0.7	0.1	-0.2	5.0	0.2	-0.1	0.1
1	8.5	0.8	0.1	-0.1	1.9	-0.5	-0.3	-0.1
4	8.5	0.9	0.3	0.1	1.0	-0.6	-0.3	-0.1

TABLE 6 Delay % error with lumped circuit (same direction, E_2=0 drive case)

	n=1				n=2			
η	N=1	N=2	N=3	N=5	N=1	N=2	N=3	N=5
0.01	8.6	1.1	0.3	0.2	8.6	1.0	0.3	0.2
0.1	8.6	1.0	0.3	0.1	8.6	1.0	0.2	0.1
0.4	9.4	1.3	0.4	0.0	10.1	1.6	0.6	0.1
1	11.6	2.6	1.0	0.3	14.2	3.3	1.2	0.3
4	20.3	8.1	4.0	1.3	29.1	7.7	3.0	0.8

8. Conclusion

Simple yet useful analytical expressions for peak noise amplitude, delay and slope for capacitively coupled two-, three- and infinite-line systems.

The calculated results using the derived formulas of (7), (14) for the crosstalk noise and (6), (8), (16) for the delay and the slope coincide excellently with SPICE simulation results. The derived approximate expressions like (9), (15) and (17) are useful in estimating the crosstalk noise and delay in the early stage of designs and give insight to coupling related issues.

In deep submicron VLSI designs where C_C can be comparable to C, the crosstalk induced by the coupling goes up to 40% of the signal swing and the delay fluctuates 5 times depending on the behavior of the adjacent lines.

As for the approximation with lumped circuit, 3-step π-ladder network is good approximation within 4% relative error even in the worst cases.

References

[1] H. B. Bakoglu, "Circuits, Interconnections, and Packaging for VLSI," Addison-Wesley, 1990.

[2] W. C. Elmore, "The Transient Response of Damped Linear Networks with Particular Regard to Wideband Amplifiers," J. of Applied Physics, Vol. 19, pp. 55-63, Jan. 1948.

[3] L. T. Pillage and R. A. Rohrer, "Asymptotic Waveform Evaluation for Timing Analysis," IEEE Trans. on Comp. Design, Vol. 9, No. 4, pp. 352-366, Apr. 1990.

[4] T. Quarles, A. R. Newton, D. O. Pederson and A. Sangiovanni-Vincentelli, "SPICE 3B1 User's Guide," EECS, Univ. of Calif. Berkeley, 1988.

[5] T. Sakurai, "Approximation of Wiring Delay in MOSFET LSI," IEEE J. of Solid-State Circ., Vol. 18, No. 4, pp. 418-426, Aug. 1983.

[6] T. Sakurai, S. Kobayashi, and M. Noda, "Simple Expressions for Interconnection Delay, Coupling and Crosstalk in VLSI's," Int. Symp. on Circ. and Systems, Singapore, pp. 2375-2378, June 1991.

[7] T. Sakurai, "Closed-Form Expressions for Interconnection Delay, Coupling and Crosstalk in VLSI's," IEEE Trans. on Electron Devices, Vol. 40, No. 1, pp. 118-124, Jan. 1993.

[8] T. Sakurai and K. Tamaru, "Simple Formulas for Two- and Three-Dimensional Capacitances," IEEE Trans. on Electron Devices, Vol. 30, No. 2, pp. 183-185, Feb. 1983.